Biochimica et Biophysica Acta 1841 (2014) 1733–1740

Contents lists available at ScienceDirect

Biochimica et Biophysica Acta

journal homepage: www.elsevier.com/locate/bbalip

Characterization of fatty acid binding and transfer from Δ98Δ, a functional all-β abridged form of IFABP

Luciana Rodriguez Sawicki [a], María Ximena Guerbi [a], Lisandro Jorge Falomir Lockhart [a], Lucrecia María Curto [b], José María Delfino [b], Betina Córsico [a], Gisela Raquel Franchini [a,*]

[a] Instituto de Investigaciones Bioquímicas de La Plata (INIBIOLP), CCT-La Plata (CONICET), Facultad de Cs. Médicas (UNLP), Calle 60 y 120, 1900 La Plata, Argentina
[b] Department of Biological Chemistry and Institute of Biochemistry and Biophysics (IQUIFIB), School of Pharmacy and Biochemistry, University of Buenos Aires, Junín 953, C1113AAD Buenos Aires, Argentina

ARTICLE INFO

Article history:
Received 23 June 2014
Received in revised form 15 September 2014
Accepted 30 September 2014
Available online 13 October 2014

Keywords:
Intestinal fatty acid binding protein
β-Barrel
Protein truncation
Ligand binding
Membrane interaction
Model membranes

ABSTRACT

Intestinal fatty acid binding protein (IFABP) is an intracellular lipid binding protein whose specific functions within the cell are still uncertain. An abbreviated version of IFABP encompassing residues 29–126, dubbed Δ98Δ is a stable product of limited proteolysis with clostripain of holo-IFABP. Cumulative evidence shows that Δ98Δ adopts a stable, monomeric and functional fold, with compact core and loose periphery. In agreement with previous results, this abridged variant indicates that the helical domain is not necessary to preserve the general topology of IFABP's β-barrel and that the helix-turn-helix motif is a fundamental element of the portal region involved in ligand binding and protein–membrane interactions. Results presented here suggest that Δ98Δ binds fatty acids with affinities lower than IFABP but higher than those shown by previous helix-less variants, shows a 'diffusional' fatty acid transfer mechanism and it interacts with artificial membranes. This work highlights the importance of the β-barrel of IFABP for its specific functions.

1. Introduction

Intestinal fatty acid-binding protein (IFABP) belongs to a family of intracellular lipid binding proteins of low molecular mass (14–15 kDa) with the putative general function of lipid trafficking [1]. The precise physiological functions of these proteins are as yet not precise, but it is hypothesized that they may have a central role in intracellular transport and targeting of fatty acids (FA) to specific membranous organelles and metabolic pathways [2]. IFABP is abundantly produced in the enterocyte, where a second FABP, liver-type FABP (LFABP), is also highly expressed [3,4]. A number of differences between the two enterocyte FABPs have been described, including binding specificity, stoichiometry, mode of ligand transport and membrane interaction properties, suggesting unique functional properties [5–8]. Remarkably, all FABPs share an almost superimposable β-barrel fold that resembles a clamshell. This β-barrel consists of ten β-strands (A–J) arranged in two nearly orthogonal β-sheets that enclose the ligand binding cavity [9,10]. The barrel is capped with a helix-turn-helix motif located between strands βA and βB. This helical subdomain has been described as the portal region together with residues from βC-D and βE-F connecting loops, and it is hypothesized that it may regulate the entry of FA into the cavity [11]. This characteristic tertiary structure differs from most globular proteins since its interior is occupied by a large solvent-filled cavity, while the hydrophobic core is small and displaced from the protein center. The key to a better understanding of the unique functions of these FABPs may rely on the structural characterization and, therefore, on a detailed structure–function analysis of the subdomains found in their fold.

To address the possible binding and transport functions of IFABP at the structural level, previous works have focused on a series of structural variants of this protein and of other members of the FABP family. Through the years, these works have highlighted the importance of different regions of FABPs involved in functional processes like ligand binding and transfer of its cargo to artificial membranes. It was the helix-turn-helix motif that received particular attention regarding ligand binding and ligand transfer mechanisms to model phospholipid membranes. Using fast kinetics measurements, it has been demonstrated that transfer of FA from IFABP to membranes appears to occur during direct collisional interactions between the protein and the

Abbreviations: FABP, fatty acid binding protein; IFABP, intestinal fatty acid binding protein; LFABP, liver fatty acid binding protein; wtIFABP, wild-type intestinal fatty acid binding protein; wtLFABP, wild-type liver fatty acid binding protein; Δ98Δ, a truncated variant of IFABP corresponding to the fragment 29–126 of the parent protein; Δ17-SG, an abbreviated form of IFABP engineered by deleting 17 residues that span the helical domain and replacing them by a Ser–Gly linker; apo- or holo-, prefixes that denote the absence or presence of fatty acid ligand; FA, fatty acids; SUVs, small unilamellar vesicles; AOFA, anthroyloxy-labeled fatty acid; 12AO, 12- (9-Anthroyloxy)oleic acid; 12AS, 12- (9-Anthroyloxy)stearic acid; EPC, egg phosphatidylcholine; NBD-PC, egg N-(7-nitro-2,1,3-benzoxadiazol-4-yl) phosphatidylcholine; CL, bovine heart cardiolipin

* Corresponding author. Tel.: +54 221 4824894; fax: +54 221 425 8988.
E-mail address: gfranchini@conicet.gov.ar (G.R. Franchini).

http://dx.doi.org/10.1016/j.bbalip.2014.09.022
1388-1981/

acceptor membrane, while LFABP transfers FA to acceptor membranes in a diffusional manner, involving an initial release of the ligand to the aqueous milieu prior to its membrane association [5,7,12].

IFABP is a useful model to study the structure and dynamics of β-sheet proteins. In order to get further knowledge about IFABP folding process, identify possible nucleation events and determine the importance of the α-helical region, two consecutive variants of helix-less IFABP (Δ17-SG and Δ27-GG) were constructed and analyzed, showing that the helical domain is not necessary to preserve the general topology of IFABP [13,14]. Interestingly, these proteins retain the ability to bind fatty acids, although with a lower affinity than the full-length protein, indicating that the helical domain contributes to regulate the affinity of the protein for different FA. More recently, a novel abbreviated helix-less variant of IFABP was obtained as a stable product of limited proteolysis of this protein with clostripain (Arg-C) in the presence of oleate as ligand [15]. Remarkably, the main fragment generated after proteolysis with clostripain of holo-IFABP is highly resistant to further degradation. It was then postulated that stability to proteolysis of this 11 kDa fragment (dubbed Δ98Δ) is due to its ability to bind the ligand, a feature that would help it remain structured. Hence, this is the first helix-less variant not rationally designed, but rather obtained through a 'protease selection' process. Δ98Δ variant lacks the first β-strand (βA) and most of the helix-turn-helix domain, as well as the last four residues of βJ (Fig. 1). Structural and binding analyses show that Δ98Δ folds properly, adopting the classical β-barrel structure, and maintaining ligand binding capacity [15].

In order to get further insight into Δ98Δ functional capabilities, we extensively studied the binding affinities of this protein for natural and fluorescent tagged FA and we analyzed the rate and mechanism of fluorescent tagged FA transfer to membranes of different compositions. On the other hand, we studied the ability of Δ98Δ to physically interact with membranes employing different approaches. We used an acrylamide quenching assay, an ultracentrifugation assay and a terbium leakage experiment. This work demonstrates that Δ98Δ, not only retains its ability to bind FA, but also interacts with phospholipid membranes although displaying a diffusional FA transfer mechanism. This is in agreement with the sequential FA transfer mechanism hypothesis proposed for IFABP where other regions of the protein would be able to interact with membranes even in the absence of the leading helix-turn-helix motif [16].

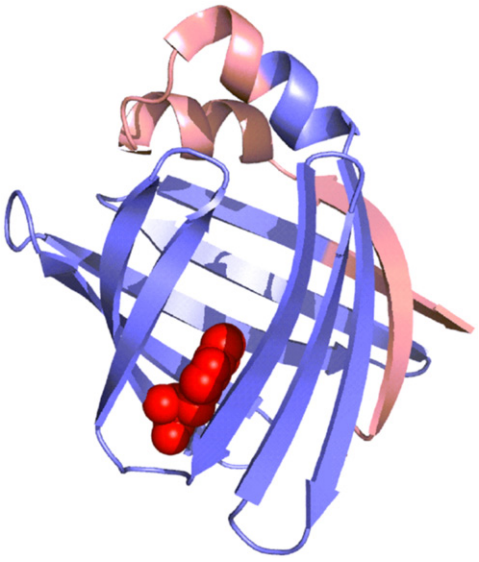

Fig. 1. Ribbon structure of IFABP (PDB 2IFB) where the Δ98Δ construct is indicated. The excised N- and C-termini are shown in pink, Δ98Δ in light blue, and the only W present in Δ98Δ is shown in red.

2. Materials and methods

2.1. Materials

Sodium oleate was obtained from Nu-Chek Prep (Elysan, MN). Anthroyloxy fatty acids (AOFA), 12-(9-anthroyloxy)-oleic acid (12AO) and 12-(9-anthroyloxy)-stearic acid (12AS), and acrylodated IFABP (ADIFAB) were purchased from Molecular Probes, Inc. (Eugene, OR). Egg phosphatidylcholine (EPC), N-(7-nitro-2,1,3-benzoxadiazol-4-yl) phosphatidylcholine (NBD-PC), and bovine heart cardiolipin (CL) were obtained from Avanti Polar Lipids (Alabaster, AL). Lipidex-1000, acrylamide, Terbium (III) chloride and dipicolinic acid (DPA) were purchased from Sigma-Aldrich (St. Louis, MI). All other chemicals were reagent grade or better.

2.2. Protein expression and purification

Rat wild type IFABP (wtIFABP) cDNA, coded in the plasmid pET-11a, was expressed in *Escherichia coli* strain BL21(DE3). The structural variant lacking the α-helical domain (Δ17-SG) was overexpressed in *E. coli* harboring pMON-IFABPHL [17]. Both proteins were purified from *E. coli* as described previously [5,17]. Purification of recombinant Δ98Δ was performed as detailed in Curto et al. 2005 [15] with subtle modifications. Briefly, cells were lysed by sonication. After dissolution of the inclusion bodies in buffer A (10 mM potassium phosphate, 150 mM KCl, pH 7.4) supplemented with 5 mM glycine and 2 M urea, the sample was centrifuged (27,000 *g* for 20 min at 4 °C) and the supernatant applied to a Sephadex G-50 column (50 cm length by 4.5 cm diameter) equilibrated and eluted with buffer A. Subsequently, fractions containing Δ98Δ were pooled and sampled onto an anion exchange column (Whatman DE-52, 2.5 cm length by 3 cm diameter). Elution was carried out in a single step with buffer A supplemented with 100 mM NaCl. The eluted protein was dialyzed against buffer A. Purified protein was delipidated by passage through a Lipidex 1000 column (Sigma, 35 cm by 1 cm) at 37 °C using buffer A. Purity was assessed in SDS-PAGE gels. Finally, pooled fractions containing the concentrated proteins were stored at −80 °C. Protein concentration was assessed by spectrophotometer measurements at 280 nm with the corresponding extinction coefficients: $\varepsilon = 16{,}900\ M^{-1}\ cm^{-1}$ for IFABP and Δ17-SG; and $\varepsilon = 9153\ M^{-1}\ cm^{-1}$ for Δ98Δ.

2.3. Ligand binding assays

2.3.1. Binding of natural ligands

The binding of oleate was analyzed using the fluorescent probe ADIFAB employing a competition assay as described before [18]. Briefly, this assay allows for the direct measurement of unbound FA in equilibrium with the FABP studied and the probe. Protein concentrations were 10 μM Δ98Δ, 4 μM wtIFABP or 10 μM Δ17-SG with 0.2 μM ADIFAB. The stock solution used to perform the titration of the protein samples was 25 mM sodium oleate in 10 mM HEPES, 150 mM NaCl, 5 mM KCl, 1 mM Na_2HPO_4 pH 7.4 buffer and it was incubated at 37 °C while performing the assay. Measurements were performed using a Fluorolog-3 Spectrofluorometer (Horiba-Jobin Yvon, France) employing experimental parameters suggested by the manufacturer of the probe (λex = 383 nm; emission scan from 400 to 520 nm). To estimate the K_D values, a single-site Scatchard analysis was employed.

2.3.2. Binding of fluorescent fatty acid analogs

Binding of anthroyloxy-FA (AOFA) to IFABP, Δ17-SG and Δ98Δ was assessed by measuring changes in the intensity of fluorescence emission of the FA analog with increasing concentrations of protein [19]. Briefly, 0.5 μM AOFA was incubated at 25 °C for 3 min in 40 mM Tris HCl, 100 mM NaCl, pH 7.4 buffer (TBS) with increasing concentrations of IFABP, Δ17-SG or Δ98Δ. The AOFAs employed for binding assays were

12-(9-anthroyloxy) stearic acid (12AS) and 12-(9-anthroyloxy) oleic acid (12AO). Fluorescence emission at 437 nm was registered after excitation at 383 nm. Measurements were performed in a Fluorolog 3 Spectrofluorometer. Dissociation constants (K_D) were calculated by employing a single-site Scatchard analysis.

2.4. Preparation of model membranes

Small Unillamellar Vesicles (SUVs) were prepared by sonication and ultracentrifugation as described previously [20]. The standard vesicles were prepared to contain 90 mol% of EPC and 10 mol% of NBD-PC. The NBD moiety works as a Förster Resonance Energy Transfer (FRET) acceptor of the anthroyloxy group (donor). To increase the negative charge density of the acceptor vesicles, 25 mol% of CL was incorporated into the SUVs in place of an equimolar amount of EPC Vesicles that were prepared in TBS buffer except for SUVs containing CL, which were prepared in TBS with 1 mM EDTA.

Large Unilamellar Vesicles (LUVs) were prepared as described before [21]. Briefly, multilamellar vesicles of 100% EPC or EPC:CL (3:1) were prepared (0.5 mM phospholipids) by mixing the lipids in chloroform, drying them under a stream of N_2, and resuspending them in TBS by vortexing. Sucrose (180 mM) was added when preparing LUVs for the sucrose loaded vesicle-binding assay. For CL containing vesicles, TBS also had 1 mM EDTA included. Then lipid suspensions were incubated at 37 °C for 30 min and passed 11 times through the polycarbonate filters using a Liposofast Extruder System (Avestin) to obtain the LUVs of uniform size of approximately 100 nm.

SUVs for Tb leakage assay were prepared according to the method of Wilschut et al. [22].

2.5. Relative partition coefficient measurement

The relative partition coefficient (K_P) for AOFA partitioning between wtIFABP, Δ17-SG or Δ98Δ and SUVs allows us to obtain a measurement of relative affinity of the different structural variants for their ligands in the presence of acceptor SUVs. It was determined by measuring AOFA fluorescence at a given molar ratio of protein:SUV after titration of SUVs into a solution containing the preformed complex (0.5 μM 12AO with 5 μM IFABP or 20 μM Δ17-SG or Δ98Δ in TBS at 25 °C) [23].

$$K_P = \frac{[\text{SUV bound AOFA}].[\text{FABP}]}{[\text{SUV}].[\text{FABP bound } AOFA]}. \quad (1)$$

The decrease in AOFA fluorescence upon titration with SUVs containing NBD-PC was related to K_P by the following equation:

$$\frac{1}{\Delta F} = \frac{1}{K_P}\cdot\frac{1}{\Delta F_{max}}\cdot\frac{[\text{FABP}]}{[\text{SUV}]} + \frac{1}{\Delta F_{max}} \quad (2)$$

where ΔF is the difference between the initial fluorescence of AOFA in the protein and the AOFA fluorescence at a given protein:SUV ratio, and ΔF_{max} is the maximum difference in AOFA fluorescence. A plot of $1 / \Delta F$ versus $(1 / \Delta F_{max}) \times ([\text{FABP}] / [\text{SUV}])$ gives a slope of $1 / K_P$.

2.6. Transfer of fluorescently labeled fatty acids from proteins to SUVs

A FRET assay was employed to monitor the transfer of 12AO or 12AS from Δ98Δ to acceptor model membranes as described in detail elsewhere [5,17,19]. Briefly, each protein with bound AOFA was mixed at 25 °C with SUVs using a stopped-flow spectrofluorometer RX-2000 (Applied Photophysics Ltd., UK). Upon mixing, the ligand is transferred to the liposomes and AOFA fluorescence is quenched by the NBD-PC. Transfer of AOFA from protein to membrane is directly monitored by the time-dependent decrease in the anthroyloxy group fluorescence.

Binding constants (K_D) and partition coefficients (K_P) were employed to establish AOFA transfer assay conditions so as to ensure a low level (‹4%) of unbound fatty acid concentration at time zero in the transfer experiments and an essentially unidirectional transfer from proteins to membranes. Final transfer assay conditions were 15 μM wtIFABP with 1.5 μM AOFA and 150–600 μM SUV or 45 μM Δ17-SG or Δ98Δ with 0.75 μM AOFA and 150–1200 μM SUV. Controls to ensure that photobleaching was not significant were performed prior to each experiment [17]. Data were analyzed by averaging at least 5 reproducible consecutive runs and fitting a single exponential decay model to the resulting data. All curves were well described by a single exponential function. For each data point, at least three independent measurements were performed. Average values ± S.E.M. for three or more separate experiments are reported.

2.7. Sucrose loaded vesicle binding assay

We employed sucrose loaded LUVs to explore binding of FABPs as described in Smith and Storch [24]. Briefly, reactions of LUVs and FABPs were prepared in binding buffer (200 μl; 5 mM MOPS, pH 7.4, 100 mM KCl, 2 mM $CaCl_2$). Tubes were centrifuged at 100,000 *g* for 90 min at 21 °C, and the supernatant was immediately transferred to new tubes. Portions of both supernatant and pellet were resolved by SDS-PAGE.

Gel densitometry was analyzed using the gel analyzer tool of Image J software (http://imagej.nih.gov/ij/).

2.8. Acrylamide quenching

Trp fluorescence emission spectra were recorded from 300 to 400 nm, with excitation wavelength set at 295 nm to prevent excitation of the tyrosine residues. The excitation slit width was set to 4 nm and the emission slit width to 8 nm. The protein concentration employed was 5.0 μM and the LUV concentration was 40 μM. For the quenching experiments, acrylamide was added from a 4.0 M stock solution to the protein solution from 0 to 400 mM. After each addition, the samples were equilibrated for 3 min at 25 °C before the spectrum was recorded. Fluorescence quenching experiment data was analyzed according to the Stern–Volmer equation:

$$\frac{F_0}{F} = 1 + \text{Ksv}.[Q] \quad (3)$$

where F_0 and F are the integrated emission intensities in the absence or in the presence of the quencher Q, respectively, and K_{SV} is the Stern–Volmer constant [25].

2.9. Terbium leakage assay

Stock suspensions of FABP and SUVs, loaded with the Tb/DPA complex in their internal aqueous spaces, were prepared in 20 mM Tris HCl (pH 8.0), 155 mM NaCl 12.5 mM EDTA to eliminate osmotic effects. These working solutions were mixed and the fluorescence signal of Tb/DPA complex was monitored, with excitation set at 250 nm and emission at 545 nm. Induced leakage by FABP interaction with the membranes was monitored as the decrease in Tb fluorescence since EDTA replaces DPA in the complex. Data were expressed as percent of the total disruption of the vesicles with 0.05% Triton X-100 and calculated as follows:

$$\%\,\text{of induced leakage} = 100\cdot\frac{F_b - F}{F_b - F_t} \quad (4)$$

where F and F_b are, respectively, the fluorescence intensity signals for the sample and for the blank (vesicles mixed with the corresponding buffer) and F_t is the fluorescence intensity obtained measured for the addition of the detergent solution to the lipid vesicles [22].

3. Results

3.1. In vitro binding of fatty acids to Δ98Δ

Δ98Δ is the smallest monomeric variant of IFABP described so far that maintains a β-barrel-like structure capable of binding FAs [15]. We used the fluorescent probe ADIFAB, an IFABP covalently modified with an acrylodan fluorophore, to assess the equilibrium binding affinity of Δ98Δ for oleate. Binding of FAs to ADIFAB induces a red shift in the acrylodan emission spectrum. Therefore the ratio of fluorescence intensity emitted at 505 to that at 432 nm reflects the fraction of bound ADIFAB and this is used to provide a measure of unbound FA in solution in equilibrium with the investigated protein. Using the known K_D of ADIFAB for oleic acid [18], one can determine the corresponding K_D of another protein. The K_D obtained for wtIFABP was 0.03 ± 0.02 μM (see Supplementary data), which is in agreement with previous reports [16,18]. Data for the structural variants demonstrated that Δ98Δ and Δ17-SG bind oleate, though with lower affinity than wtIFABP (0.57 ± 0.39 μM and 4.26 ± 0.23 μM, respectively) (see Supplementary data). It is important to note that Δ98Δ presents a higher affinity for oleate than Δ17-SG.

Complementary to the previous assay, we analyzed the binding of AOFAs: 12AO and 12AS. The spectral properties of anthroyloxy probes are sensitive to their immediate environment so they can be useful indicators of binding site characteristics. These probes usually show very low fluorescence intensity in buffer, which becomes dramatically enhanced upon interaction with the hydrophobic binding subdomain of a FABP [26]. As shown in Fig. 2, both, 12AO and 12AS, show a large increase in fluorescence emission when bound to Δ98Δ. Fig. 2A shows the blue shift of the emission spectra of 12AO bound to Δ98Δ. The observed changes indicate a considerably more constrained environment for the anthroyloxy moiety when bound to the protein [26], suggesting that the probe is located in a hydrophobic pocket. The blue shift in the spectra is more important for 12AO than for 12AS, this difference could be due to a different microenvironment observed by the fluorescent moiety of the AOFA. Given that the acyl carbon chain of 12AO presents a double bond that introduces a kink in the acyl chain, the anthroyloxy group might be accommodated in a different manner within the binding cavity of Δ98Δ. In both cases (12AO and 12AS) ligands bind to the protein in a saturable manner (Fig. 2C and D) and with a 1:1 stoichiometry. The K_D values obtained using a Scatchard analysis are K_D (12AO) = 0.6 ± 0.1 μM and K_D (12AS) = 0.9 ± 0.3 μM.

3.2. Relative partition coefficient measurements

An apparent partition coefficient value was also obtained for each protein, describing the relative distribution of 12AO and 12AS between FABP and EPC-SUVs. The partition coefficients obtained are shown in Table 1. Analysis of these data showed a preferential partitioning of 12AO to SUVs relative to wtIFABP while the saturated ligand 12AS partitions toward the protein, in accordance with previous results reported [16,27] and with the dissociation constants of natural ligands that indicate wtIFABP has a higher affinity for stearic over oleic acid [18].

Δ98Δ showed similar K_P values partitioning of both, 12AO and 12AS ligands. Results obtained showed an almost equivalent distribution of both AOFAs between protein and membrane meaning that there is no difference in affinity for both assayed ligands. This is in agreement with the abovementioned K_D values obtained for AOFAs. On the other hand, the partitioning of both AOFAs between Δ17-SG and vesicles showed a clear tendency of AOFA to partition toward membranes. In this case, the K_P values were clearly higher than those observed for wtIFABP or Δ98Δ. This is in agreement with the observation that Δ17-SG presents lower affinity for ligands when compared with Δ98Δ [17].

All further studies were performed under conditions where the acceptor to donor ratios (FABP:SUV) were above the determined equilibrium partition coefficients (Table 1) in order to ensure uniformly unidirectional transfer in kinetic experiments [5].

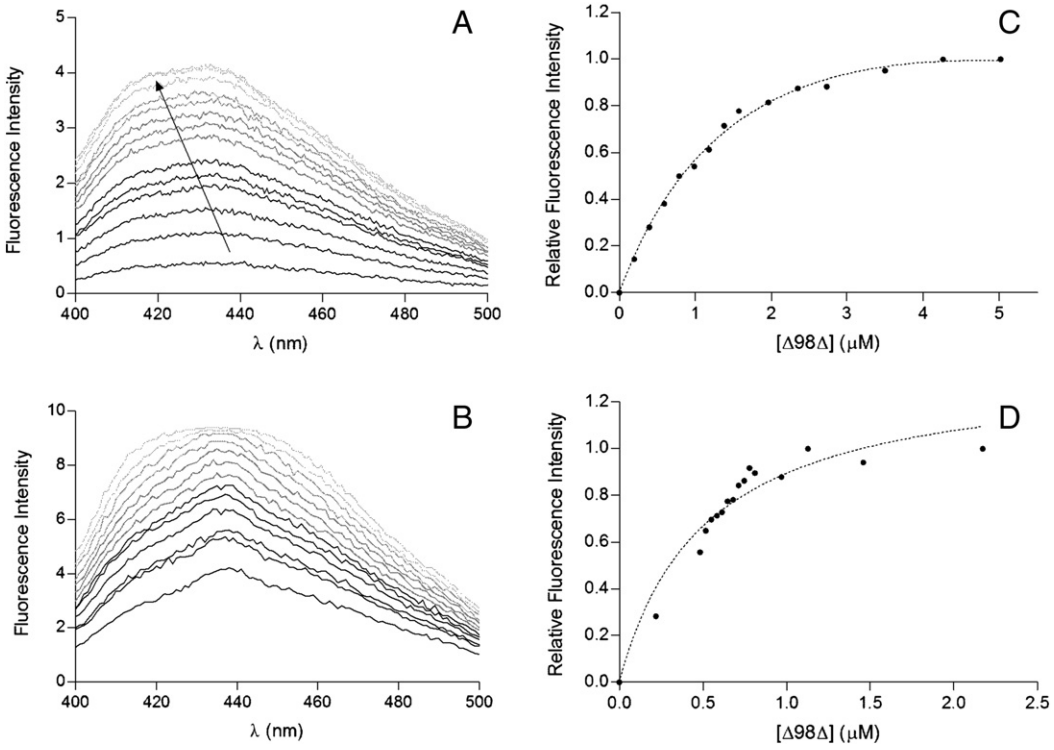

Fig. 2. Emission spectra of 12AO (A) and 12AS (B) bound to Δ98Δ. Changes in relative fluorescence of both AOFAs were monitored from 400 to 500 nm after excitation at 383 nm. Binding isotherms showing changes in relative fluorescence at 440 nm of the complex Δ98Δ-12AO (C) and Δ98Δ-12AS (D) were obtained by fluorimetric titration.

Table 1
Comparison of partition coefficient of 12AO and 12AS. K_P units (μM FABP / μM SUV).

	K_P 12AO	K_P 12AS
wtIFABP	8 ± 2	0.53 ± 0.04
Δ98Δ	1.03 ± 0.09	1.1 ± 0.1
Δ17-SG	11 ± 4	21 ± 6

3.3. Effect of acceptor membrane concentration on AOFA transfer from Δ98Δ

The effect of acceptor membrane concentration on rates of ligand transfer has been used to distinguish between an aqueous diffusion mechanism, where no effect is observed, and a collision-mediated mechanism, where the ligand transfer rate would be directly related to the donor–acceptor collisional frequency and, hence, to the vesicle concentration [19]. wtIFABP is a well characterized example of a FABP with a collisional ligand transfer mechanism. To investigate whether the FA transfer mechanism of Δ98Δ was affected, the AOFA transfer from this variant to model zwitterionic membranes was examined as a function of increasing SUV concentration, and results compared to those for the wtIFABP. The results in Fig. 3A and B, show that 12AO and 12AS transfer from Δ98Δ is essentially unaffected by acceptor vesicle concentration. Conversely, both ligands transfer rate from wtIFABP to NBD-EPC SUV increases proportionally as a function of vesicle concentration, in accordance with a collisional transfer mechanism. Previous works have pointed out the centrality of the α-helical region in determining the ligand transfer mechanism in the so called "collisional" FABPs [17,19,28]. It now becomes clear that the lack of the missing (1–28 and 127–131) stretches affects the mechanism of FA transfer from Δ98Δ to model membranes.

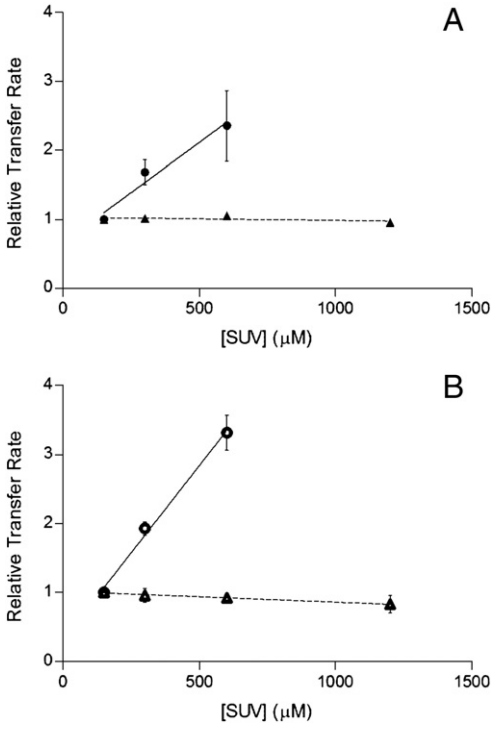

Fig. 3. Effect of acceptor membrane concentration on the transfer of AOFA from FABP. (A) Transfer of (●) 1.5 μM 12AO from 15 μM wtIFABP to EPC/NBD-PC SUVs and (▲) 0.75 μM 12AO from 45 μM Δ98Δ to EPC/NBD-PC SUVs. (B) Transfer of (O) 1.5 μM 12AS from 15 μM wtIFABP to EPC/NBD-PC SUVs and (Δ) 0.75 μM 12AS from 45 μM Δ98Δ to EPC/NBD-PC SUVs. Average transfer rates from three different experiments ± the standard deviation are shown in both graphs.

3.4. Effect of phospholipid charge on AOFA transfer from FABP to membranes

The hypothesis that FA transfer from wtIFABP occurs during collisional contact with an acceptor membrane implies that membrane properties could potentially modulate the rate of transfer. By contrast, in the case of aqueous diffusion, characteristics of the acceptor membrane would not be expected to regulate the transfer rate, since the rate-determining step in the transfer process – ligand dissociation from the protein into the aqueous phase – is a temporally distinct event from processes involving the acceptor membrane. Fig. 4 shows that, as expected from previous studies, the rate of transfer of 12AO from wtIFABP is substantially increased by incorporation of 25 mol% CL into NBD-EPC acceptor membranes, whereas transfer of 12AO from Δ17-SG was essentially unaffected by the presence of negatively charged phospholipids [17,19]. The results for Δ98Δ resemble completely those for Δ17-SG, further implying that the mechanism of the transfer of FA from Δ98Δ is likely a diffusional process.

3.5. Sucrose loaded vesicles

We employed a differential centrifugation method to examine interfacial membrane binding of FABPs to sucrose loaded LUVs of different compositions. Protein–membrane interaction is monitored by analyzing the modification in the quantity of unbound protein when LUVs are incorporated. Fig. 5A shows a single experiment using wtIFABP, wtLFABP and Δ98Δ in their apo-forms; before and after incubation with 100% EPC LUVs. wtLFABP and Δ98Δ presented a very slight decrease in band intensity while wtIFABP showed almost no change in the presence of EPC vesicles. According to densitometry quantification, Δ98Δ showed the lowest percentage of protein remaining in the supernatant (see Table 2), suggesting that there are different degrees of interaction for these proteins. Fig. 5B shows the incubation of the same set of proteins with 25% CL-containing LUVs. This time a clear decrease was observed in the presence of negatively charged vesicles (see Table 2). Since this assay is performed at equilibrium, these results are in agreement with transient complexes formed when incubated with zwitterionic LUVs, as previously reported [16]. Notably, when negative charges are incorporated into membranes this equilibrium is shifted toward a more stable protein adsorption to the LUVs. Remarkably, Δ98Δ interacts with both types of LUVs and this interaction seems to be markedly enhanced by a negatively charged surface.

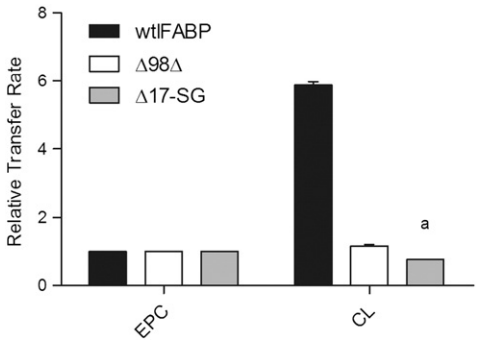

Fig. 4. Effect of vesicle charge on transfer of AOFA from FABP. Transfer of 1.5 μM 12AO from 15 μM wtIFABP to 150 μM EPC/NBD-PC SUVs containing 25 mol% CL, 0.75 μM 12AO from 45 μM Δ98Δ to 150 μM EPC/NBD-PC SUVs containing 25 mol% CL, or 0.75 μM 12AO from 45 μM Δ17-SG to 150 μM EPC/NBD-PC SUVs containing 25 mol% CL. Results are expressed relative to the rate of transfer of 12AO to EPC/NBD-PC membranes. Averages from three different experiments ± the standard deviation are shown. The letter a indicates that a single transfer experiment was done.

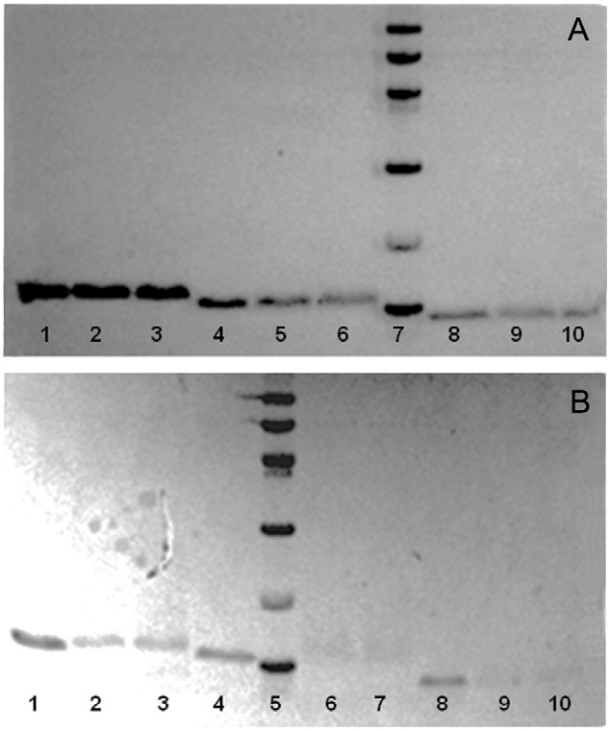

Fig. 5. Binding of intestinal FABPs to sucrose loaded LUVs. The stable binding of apo-FABP to LUVs of 100% EPC (A) or 25% CL (B) was analyzed by differential ultracentrifugation. Lines 1, 4 and 8 of each gel are purified wtIFABP, wtLFABP and Δ98Δ, respectively, incubated in the absence of LUVs. (A) The consecutive two lines after each purified protein are replicates of the same experiment of unbound protein in the supernatant after ultracentrifugation in the presence of LUVs. (B) Lines 2 and 3, lines 6 and 7 and lines 9 and 10 are replicates of the same experiment of unbound protein in the supernatant after ultracentrifugation in the presence of LUVs for wtIFABP, wtLFABP and Δ98Δ respectively.

3.6. Acrylamide quenching

In order to get further information on Δ98Δ interaction with membranes, changes in Trp fluorescence in the presence or in the absence of EPC LUVs were analyzed. Quenching by acrylamide is mainly a collisional effect and is thus dependent on the concentration of quencher and the solvent accessibility of the Trp residue. Δ98Δ preserves only one Trp and it corresponds to Trp82 of wtIFABP, which is placed at the bottom of the β-barrel and is part of the hydrophobic core (Fig. 1). Additionally, the results presented here were further compared with previous reports by our group, on W6F, an IFABP point mutant where W6 was exchanged for Phe and only W82 remains [25]. The obtained Stern–Volmer constants (K_{SV}) are summarized in Table 3. In the absence of LUVs, K_{SV} values for Δ98Δ and W6F are indistinguishable, indicating that Trp82 may be similarly exposed in both variants. These results also give evidence for a well preserved β-barrel for Δ98Δ. A straightforward comparison with wtIFABP is more complicated since Trp6 and Trp82 are both present and contribute to the emission spectra (although the quantum yield of fluorescence emission for Trp6 is significantly lower).

Table 2
Binding of FABPs to sucrose loaded LUVs. Percentage of FABP in the supernatant after centrifugation.

	EPC	EPC-CL
wtIFABP	93.5 ± 7.1	23.6 ± 4.7
wtLFABP	74.2 ± 9.7	22.9 ± 4.8
Δ98Δ	58.1 ± 0.1	15.4 ± 2.8

Table 3
Acrylamide quenching of proteins in the presence and absence of LUVs.

	$K_{SV\ buffer}$[a]	$K_{SV\ LUVs}$[a]
wtIFABP[b]	4.3 ± 0.4	4.7 ± 0.3
Δ98Δ	8.5 ± 0.5	4.4 ± 0.4
W6F[b]	7.7 ± 1.1	5.1 ± 1.3

[a] K_{SV} results are average of at least 3 independent measurements ± SEM. Units are μM^{-1}.
[b] Data already published by our group in De Geronimo et al. 2014. Experiments were all performed at the same time.

In the presence of LUVs, K_{SV} values for Δ98Δ and W6F are diminished, showing a more protected environment for Trp82 in this situation. These results could be indicating that – although lacking the α-helical subdomain – Δ98Δ could still be interacting through β-barrel elements and hence restricting the access of acrylamide to the binding cavity. wtIFABP K_{SV} value is the weighted average of W6 and W82 contributions in the presence or in the absence of LUVs, and there is no change observed in presence of model membranes.

3.7. Terbium leakage assay

The effect of FABPs on membrane structure was assessed by analyzing the ability of these proteins to induce leakage of the Tb/DPA fluorescent complex from the internal aqueous space of SUVs. This methodology has proven to be efficient in protein–membrane interaction analysis [22]. Fig. 6 shows the effect of wtIFABP and two structural variants in their apo-forms, on EPC LUVs. A 5% leakage was observed when Δ98Δ was assayed. This value is significantly lower than the 15.7% exerted by wtIFABP. On the other hand, Δ17-SG was included as a control and did not induce destabilization of membrane (Fig. 6). Altogether, these results on leakage induction from vesicles indicate that wtIFABP can destabilize phospholipid membranes and so does Δ98Δ, but to a lesser degree. In agreement with previously published data [25], a relatively deep penetration of wtIFABP segments could be suggested by the partial leakage of the internal aqueous content. An interesting observation is that 100% leakage is not reached, indicating that no stable pore is formed in the vesicles with any of the proteins.

4. Discussion

As described previously, Δ98Δ lacks the N-terminal 1–28 stretches and the last five amino acids belonging to the C-terminus, however it retains its β-sheet content, remains monomeric and is capable of binding FAs [15]. Remarkably, this abridged variant retains all the critical residues of the hydrophobic core that are assumed to be implicated in the nucleation event leading to the folded state. But the most striking feature about Δ98Δ is that, unlike Δ17-SG and Δ27-GG, it's not a rationally designed helix-less variant. Moreover, it has been proposed as a

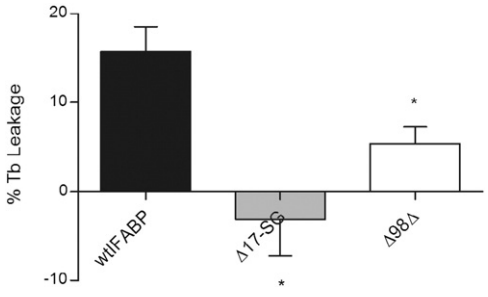

Fig. 6. Membrane destabilization by wtIFABP and its structural variants. Induced Tb/DPA complex leakage from SUVs (0.5 mM) of 100% EPC was analyzed upon mixing with FABPs (10 μM) (apo-forms). The final leakage, expressed as percentage of reference (0.05% Triton X-100), for wtIFABP, Δ17-SG and Δ98Δ is shown. Statistics was based on Student *t*-test ($p < 0.05$). * indicates significant differences between structural variants as compared to wtIFABP.

minimalist model potentially capable of populating discrete intermediates sparsely represented in the conformational ensemble of the full-length protein [29]. In this sense, we consider the use of Δ98Δ a more accurate model to test the role of the different subdomains of IFABP. In this work we complement the previous works, focused on the folding characterizations of this abbreviated variant of IFABP, and present the functional characterization of Δ98Δ, illustrating its binding properties, ligand transfer mechanism and interaction with artificial vesicles.

In the experiments presented here it has been shown that Δ98Δ binds oleic acid and fluorescent analogs of FA with lower affinities than those observed for wtIFABP, in agreement with previously published data [15,29]. In this work, K_D values for wtIFABP, Δ98Δ and Δ17-SG were determined for oleic acid using the ADIFAB probe. As expected, wtIFABP showed the highest affinity for oleic acid by comparison with both abridged variants. Remarkably, Δ98Δ showed a considerably lower K_D value when compared to Δ17-SG, giving evidence of a higher affinity for the ligand. On the other hand, K_D values for AOFAs were also measured. Results obtained for both ligands (0.6 ± 0.1 μM and 0.9 ± 0.3 μM for 12AS and 12AO respectively) are in the same order of magnitude indicating a similar affinity of Δ98Δ for both of them. When compared with previously published K_D values of IFABP and Δ17-SG for 12AO (0.16 μM and 1.7 μM, respectively) [17], Δ98Δ presents an intermediate binding constant supporting the results obtained for oleic acid. Taken together, these results could rely on the fact that Δ98Δ was first observed and identified as a proteolytic fragment of holo-IFABP, suggesting that this construct preserves all the critical interactions with the ligand. The ligand binding event would result crucial for the stabilization of side-chain contacts leading to an ultimate readjustment of the tertiary structure and determining affinities comparable with those exerted by IFABP.

The functional characterization of fatty acid binding proteins also involves the assessment of their fatty acid transfer mechanism and their interaction with membranes. Previous works using an in vitro fluorescence energy transfer assay have determined that some members of this family show a collisional transfer mechanism and some others a diffusional one [5]. For the case of Δ98Δ the absence of the 1–28 and 127–131 stretches dramatically alters the regulation of AOFA transfer from Δ98Δ. As observed in Fig. 3 the response of Δ98Δ to SUV concentration is dampened by approximately 90% when compared with wtIFABP which shows transfer rates directly proportional to vesicle concentration, a central characteristic of collision-mediated transfer processes [5,19]. Likewise, the absence of these regions results in the total loss of sensitivity of Δ98Δ to acceptor-membrane surface charge. In contrast, and as expected from the previous results, the wtIFABP demonstrates a marked enhancement of fatty acid transfer rate to acidic vesicles [5]. These results describe a diffusional FA transfer mechanism for Δ98Δ; this behavior could be associated with the absence of the alpha-helical domain which has been postulated as the leading subdomain in the collisional FA transfer mechanism [16,17,28]. Furthermore, these results are in full agreement with those observed for the Δ17-SG variant [17], providing further evidence regarding the importance of the α-helical region in conducting and determining the mechanism of FA transfer. Additionally, this is the first time that FA transfer rate is measured in the absence of the βA strand of IFABP. The comparison of the transfer behavior of both variants seems to indicate that βA is not a determinant for the collisional mechanism of transfer.

Another important aspect of IFABP function is its ability to interact with membranes. In this work we present a set of experiments – sucrose loaded vesicles, acrylamide quenching and terbium leakage assays – that were employed to analyze from different perspectives the binding of the Δ98Δ to model phospholipid membranes. The sedimentation methods and acrylamide quenching assays could be considered as techniques reporting 'long-term' or 'averaged' events since the observed results are recorded after reaching equilibrium of the different components present in the assay. In both kinds of experiments the formation of a relatively stable protein-membrane complex allowed us to monitor protein–membrane interactions. In the case of the sucrose loaded vesicles assay, all three proteins assayed showed a weak interaction with EPC membranes. Remarkably, all proteins showed a clear interaction with CL-loaded membranes suggesting that the formation of these complexes is favored by electrostatic interactions, in agreement with previously published data [7]. Additionally, the acrylamide quenching experiments showed a protective effect of the vesicles on the remaining Trp emission, yielding further evidence of the interaction of Δ98Δ with membranes. As shown in Table 3, the effect of vesicles on Δ98Δ behavior was similar to that assessed for a single Trp mutant of IFABP (W6F) which has an intact helix-turn-helix domain. The fact that these two variants behave similarly gives evidence that changes observed for Δ98Δ in the presence of vesicles are probably due to physical interaction with membranes which prevents acrylamide access to the binding cavity, and not to considerable conformational changes of Δ98Δ when is interacting with membranes. Additionally, previous works prove that the β-barrel of wtIFABP is also involved in the interaction with membranes [7,25], suggesting the existence of key elements in this subdomain for protein–membrane interaction that could be preserved in Δ98Δ. On the other hand, a Tb leakage experiment is a result of instant and irreversible ('short-term') events and, after an incubation period, we measure a sum of the individual, and possibly transient, contacts between the protein and the vesicles. Δ98Δ shows a diminished effect on membrane integrity by comparison with wtIFABP. Altogether these results show that Δ98Δ physically interacts with membranes and that this interaction may be modulated by negatively charged phospholipids. Noteworthy, Δ17-SG has never shown any interaction with membranes, neither in this work nor in previous reports when analyzed using different techniques [7,16]. The fact that Δ98Δ interacts with membranes and Δ17-SG does not, could be explained on the basis that the former variant resembles a folding intermediate and may retain several of the structural elements that are involved in the protein function.

As explained before, there is strong evidence suggesting that the α-helical region of IFABP is critical for the mechanism of ligand transfer, defining the collisional or diffusional behavior for both intestinal FABPs, as well as for the physical interaction with phospholipid membranes [17,19,28]. The fact that Δ98Δ displays a diffusional FA transfer mechanism and it also interacts with membranes might not seem an intuitive notion. Nevertheless, in the interpretation of a 'diffusional' transfer mechanism, as assessed for Δ98Δ, protein–membrane interaction should not be excluded since the rate limiting step could be the release of the ligand toward the aqueous media instead of the actual interaction with the membrane. It has been recently shown that diffusional proteins like LFABP are capable to interact physically with membranes and that this interaction is clearly modulated by the presence of the ligand [7].

In the present work, the behavior of Δ98Δ seems to correlate well with the proposed function for IFABP α-helical region as the leading interactive motif in a sequential ligand transfer mechanism. Briefly, an initial step via electrostatic interaction between the α-helical region and the membrane would be followed by a conformational change that would then promote the exit of the ligand from the binding site toward the membrane [16]. In this sense, the protein–membrane interaction results presented here suggest that, within this model mechanism, the α-helical region interaction should be further followed by the contact of the β-barrel with the membrane, and the relevance of this last step may be dependent on the lipid composition of the acceptor membrane, giving room for a molecular mechanism that would explain a directed fatty acid transport between subcellular structures.

Acknowledgements

This research has been supported by grants from the Agencia Nacional de Promoción Científica y Tecnológica (ANPCyT) (PICT26218), the Consejo Nacional de Investigaciones Científicas y Técnicas (CONICET) (PIP5773) and from the University of La Plata (UNLP) (M122).

Appendix A. Supplementary data

Supplementary data to this article can be found online at http://dx.doi.org/10.1016/j.bbalip.2014.09.022.

References

[1] J. Storch, B. Corsico, The emerging functions and mechanisms of mammalian fatty acid-binding proteins, Annu. Rev. Nutr. 28 (2008) 73–95.
[2] M. Furuhashi, G.S. Hotamisligil, Fatty acid-binding proteins: role in metabolic diseases and potential as drug targets, Nat. Rev. Drug Discov. 7 (2008) 489–503.
[3] N.M. Bass, Ligand Binding to FABP, 381985. 95–114.
[4] H. Poirier, P. Degrace, I. Niot, A. Bernard, P. Besnard, Fatty acid regulation of fatty acid-binding protein expression in the small intestine, Am. J. Physiol. 273 (1997) G289–G295.
[5] K. Hsu, J. Storch, Protein chemistry and structure: fatty acid transfer from liver and intestinal fatty acid-binding proteins to membranes occurs by different mechanisms, J. Biol. Chem. 271 (1996) 13317–13323.
[6] E. De Gerónimo, R.M. Hagan, D.C. Wilton, B. Córsico, Natural ligand binding and transfer from liver fatty acid binding protein (LFABP) to membranes, Biochim. Biophys. Acta 1801 (2010) 1082–1089.
[7] L.J. Falomir-Lockhart, G.R. Franchini, M.X. Guerbi, J. Storch, B. Córsico, Interaction of enterocyte FABPs with phospholipid membranes: clues for specific physiological roles, Biochim. Biophys. Acta 1811 (2011) 452–459.
[8] A.M. Gajda, Y.X. Zhou, L.B. Agellon, S.K. Fried, S. Kodukula, W. Fortson, K. Patel, J. Storch, Direct comparison of mice null for liver or intestinal fatty acid-binding proteins reveals highly divergent phenotypic responses to high fat feeding, J. Biol. Chem. 288 (2013) 30330–30344.
[9] J. Thompson, J. Ory, A. Reese-Wagoner, L. Banaszak, The liver fatty acid binding protein — comparison of cavity properties of intracellular lipid-binding proteins, Mol. Cell. Biochem. (February 1999) 9–16.
[10] A. Muga, D.P. Cistola, H.H. Mantsch, A comparative study of the conformational properties of *Escherichia coli*-derived rat intestinal and liver fatty acid binding proteins, Biochim. Biophys. Acta 1162 (1993) 291–296.
[11] M. Hodsdon, D. Cistola, Discrete backbone disorder in the nuclear magnetic resonance structure of apo intestinal fatty acid-binding protein: implications for the mechanism of ligand entry, Biochemistry 36 (1997) 1450–1460.
[12] H. Kim, J. Storch, Free fatty acid transfer from rat liver fatty acid-binding protein to phospholipid vesicles, J. Biol. Chem. Biol. Chem. 267 (1992) 77–82.
[13] R. Steele, D. Emmert, J. Kao, M.E. Hodsdon, C. Frieden, D.P. Cistola, The three-dimensional structure of a helix-less variant of intestinal fatty acid-binding protein, Protein Sci. 7 (1998) 1332–1339.
[14] B. Ogbay, G.T. Dekoster, D.P. Cistola, The NMR Structure of a Stable and Compact All-β-sheet Variant of Intestinal Fatty Acid-binding Protein, 2004. 1227–1237.
[15] L.M. Curto, J.J. Caramelo, M. Delfino, Δ98Δ, a functional all-β-sheet abridged form of intestinal fatty acid binding, Biochemistry 44 (2005) 13847–13857.
[16] L.J. Falomir-Lockhart, L. Laborde, P.C. Kahn, J. Storch, B. Córsico, Protein-membrane interaction and fatty acid transfer from intestinal fatty acid-binding protein to membranes support for a multistep process, J. Biol. Chem. 281 (2006) 13979–13989.
[17] B. Corsico, D.P. Cistola, C. Frieden, J. Storch, The helical domain of intestinal fatty acid binding protein is critical for collisional transfer of fatty acids to phospholipid membranes, Proc. Natl. Acad. Sci. U. S. A. 95 (1998) 12174–12178.
[18] G. Richieri, R. Ogata, A. Kleinfeld, Equilibrium constants for the binding of fatty acids with fatty acid-binding proteins from adipocyte, intestine, heart, and liver measured with the fluorescent probe ADIFAB, J. Biol. Chem. 269 (1994) 23918–23930.
[19] B. Córsico, H.L. Liou, J. Storch, The alpha-helical domain of liver fatty acid binding protein is responsible for the diffusion-mediated transfer of fatty acids to phospholipid membranes, Biochemistry 43 (2004) 3600–3607.
[20] J. Storch, A. Kleinfeld, Transfer of long-chain fluorescent free fatty acids between unilamellar vesicles, Biochemistry 25 (1986) 1717–1726.
[21] P. Hope, M.J. Bally, M.B. Webb, G. Cullis, Production of large unilamellar vesicles by a rapid extrusion procedure: characterization of size distribution, trapped volume and ability to maintain a membrane potential, Biochim. Biophys. Acta 812 (1985) 55–65.
[22] J. Wilschut, N. Düzgünes, R. Fralez, D. Papahadjopoulos, Studies on the mechanism of membrane fusion: kinetics of calcium ion induced fusion of phosphatidylserine vesicles followed by a new assay for mixing of aqueous vesicle contents, Biochemistry 19 (1980) 6011–6021.
[23] J.B. Massey, D.H. Bick, H.J. Pownall, Spontaneous transfer of monoacyl amphiphiles between lipid and protein surfaces, Biophys. J. 72 (1997) 1732–1743.
[24] E.R. Smith, J. Storch, The adipocyte fatty acid-binding protein binds to membranes by electrostatic interactions, Biochim. Biophys. Acta 274 (1999) 35325–35330.
[25] E. de Gerónimo, L. Rodriguez Sawicki, N. Bottasso Arias, G.R. Franchini, F. Zamarreño, M.D. Costabel, B. Córsico, L.J. Falomir Lockhart, IFABP portal region insertion during membrane interaction depends on phospholipid composition, Biochim. Biophys. Acta 1841 (2014) 141–150.
[26] J. Storch, N. Bass, A. Kleinfeld, Studies of the fatty acid-binding site of rat liver fatty acid-binding protein using fluorescent fatty acids, J. Biol. Chem. 264 (1989) 8708–8713.
[27] A.E.A. Thumser, J. Storch, Liver and intestinal fatty acid-binding proteins obtain fatty acids from phospholipid membranes by different mechanisms, J. Lipid Res. 41 (2000) 647–656.
[28] G.R. Franchini, J. Storch, B. Corsico, The integrity of the alpha-helical domain of intestinal fatty acid binding protein is essential for the collision-mediated transfer of fatty acids to phospholipid membranes, Biochim. Biophys. Acta 1781 (2008) 192–199.
[29] L.M. Curto, J.J. Caramelo, G.R. Franchini, J.M. Delfino, Delta98Delta, a minimalist model of antiparallel beta-sheet proteins based on intestinal fatty acid binding protein, Protein Sci. 18 (2009) 735–746.